energies

Article

Experimental Evaluation of Shale Oil Development Effectiveness by Air Injection

Chao Chen [1], Xiang Tang [2], Ming Qin [1], Rui Zhou [3,4], Zhenhua Ding [1], Guihui Lian [1], Huan Qi [3,4], Xin Chen [3,4], Zheyu Liu [3,4] and Yiqiang Li [3,4,*]

[1] Research Institute of Exploration and Development, Xinjiang Oilfield Company, Karamay 834000, China
[2] China National Oil and Gas Exploration and Development Co., Ltd., Beijing 100070, China
[3] State Key Laboratory of Petroleum Resources and Prospecting, China University of Petroleum, Beijing 102249, China
[4] Petroleum Engineering Institute, China University of Petroleum, Beijing 102249, China
* Correspondence: yiqiangli@cup.edu.cn

Abstract: In recent years, as an important part of unconventional resources, the effective development of shale oil has been a key area of research in petroleum engineering. Given the widespread availability and low cost of air, the evaluation of air injection in shale reservoirs is a topic worth exploring. This paper analyzes the production performance of different methods of air injection development in the shale reservoir, including air flooding and air huff and puff (HnP), based on full-diameter core air injection experiments. Meanwhile, the characteristics of the residual oil and produced oil are revealed by forming a systematic evaluation method that includes nuclear magnetic resonance (NMR), laser scanning confocal microscopy (LSCM), and gas chromatographic (GC) analysis. The results show that air flooding development is characterized by early gas breakthrough, long oil production period, and "L" shape oil production decline; while air HnP is characterized by first producing gas and then producing oil, rapid oil production, and high oil recovery efficiency in the first round. Compared with air flooding, the replacement efficiency of the first round of air HnP is significantly higher, demonstrating higher feasibility of air HnP in the early stages of development, although the cumulative recovery of three rounds air HnP (17.17%) is lower than that of air flooding (23.36%). The large pores (T_2 > 10 ms) are the main source of air injection recovery, while the residual oil is mainly concentrated in the medium pores (1–10 ms). Air injection development has a higher recovery factor for light components (C_{15^-}), resulting in a higher level of heavy components in the residual oil. This paper discusses the feasibility and development effectiveness of air injection in shale oil reservoirs, and its development characteristics are further clarified.

Keywords: shale oil; air flooding; air hnp; enhance oil recovery; residual oil; components

check for updates

Citation: Chen, C.; Tang, X.; Qin, M.; Zhou, R.; Ding, Z.; Lian, G.; Qi, H.; Chen, X.; Liu, Z.; Li, Y. Experimental Evaluation of Shale Oil Development Effectiveness by Air Injection. *Energies* **2022**, *15*, 9513. https://doi.org/10.3390/en15249513

Academic Editors: Dameng Liu and Albert Ratner

Received: 29 October 2022
Accepted: 23 November 2022
Published: 15 December 2022

1. Introduction

With the gradual shift from conventional to unconventional oil and gas development in recent years, gas injection has become one of the most effective means for the efficient development of tight reservoirs, which has been proven by many previous publications [1–6]. In particular, air injection development has gained more attention due to its low cost, good injection, and easy availability [7,8]. According to the development experience of air flooding in conventional oil reservoirs, air flooding is mainly suitable for light and thick oil reservoirs with high pressure and high temperature, large dip angle, and crude oil viscosity lower than 10 mPa·s [9–11]. Since 1979, Buffalo Oilfield has carried out a 19-year comparison of water injection and air injection development effects. The conclusion is that the overall air flooding effect is better, and on the basis of a certain oil price (over $25 dollars per barrel), air flooding has better economic benefits [12]. Jiang et al. (2010) combined physical and numerical simulation methods to show that the recovery factor of air flooding in low permeability reservoirs can be doubled compared to water flooding. In terms of the air flooding mechanism, it is generally believed that oxidation is crucial to the effect of air flooding, and both crude oil and rock properties directly affect the oxidation process between air and crude oil [13–15]. Meanwhile, the heat released from the oxidation reaction during air flooding causes thermal expansion of the oil along with the bond-breaking reaction of the oil, thus forming a flue gas front which results in better displacement effects in low permeability reservoirs [16,17]. Nevertheless, the thermal effect of air injection in shale oil reservoirs seems to be insignificant considering its limited air injectivity [18]. Hu et al. (2017) summarized previous cases for a comprehensive discussion on the feasibility and potential of gas injection in shale reservoirs, and concluded that factors such as micro-fractures, high-temperature and high-pressure environments, and low water content in shale oil reservoirs are conducive to air flooding, which have great potential to enhance the recovery of shale oil reservoirs [19].

Contrary to gas flooding, which would be limited by injectivity and gas channeling in tight reservoirs, gas HnP exhibits more durable and stable IOR performance [20]. In general, CO_2 and air are the two most common injection gasses, and CO_2 HnP is significantly better than air HnP due to its high solubility and diffusivity [21,22]. However, in contrast to the high production costs, severe corrosion problems, and transportation issues associated with CO_2, the air is cost-effective and non-corrosive, making air HnP a promising approach to achieving the effective development of shale oil [23,24]. The advantage of air HnP is high production efficiency and low cost in the early stage, and air HnP would form some large-contact-area gas chambers in the near-well zone that can improve the effectiveness of other high-cost solvents used later in the process [25]. Meanwhile, viscosity reduction, blocking dominant water flow channels, expanding the swept volume, and thermal flooding are considered important mechanisms to enhance shale oil recovery [26,27]. Tang et al. (2022) pointed out that when the matrix permeability is higher than 0.01×10^{-3} μm^2, gas flooding can achieve higher recovery, and vice versa, and HnP is better [28]. Recent experimental studies have shown that the air HnP has different recovery factors for different oil components, resulting in lighter components being recovered and the residual oil becoming heavier, which demonstrates the impact of air injection development on crude oil [29,30]. However, there have been limited experimental studies comparing the difference between air flooding and HnP under the same reservoir conditions, and generally, only the differences in recovery have been discussed [20]. Quantitative comparisons of production dynamics and effects on oil components of the two development models have been more rarely reported.

In this paper, for the shale oil reservoir of the Lucaogou Formation in the Jimsar area, the development characteristics of shale oil under different air injection development models (flooding and HnP) were compared with a full-diameter natural core. Combined with NMR technology, LSCM, and GC analysis, the produced oil and residual oil from air injection development in shale oil were quantitatively analyzed. This work thoroughly studied the effectiveness of air injection development in shale oil and can deepen the understanding of the air injection impacts on oil composition.

2. Experiments

Air flooding and air HnP experiments on a full-diameter core were carried out to evaluate the development characteristics of shale oil under different air injection development models. NMR and LSCM were used to analyze oil distribution and oil composition changes in the core samples, and GC analysis was used to analyze the composition changes of oil produced by different development models.

2.1. Experiment Materials

As shown in Figure 1, the cores used in the development experiments were taken from the shale reservoir of the Lucaogou Formation in Jimusar Basin, Junggar Basin, including a full-diameter core (Core J1) and two cylindrical cores (J27-1 and J27-2). The specific parameters of the cores are shown in Table 1. The oil used in the experiments was taken from the same formation, with a viscosity of 10 mPa·s at the formation temperature (85 °C). The gas used in the experiments was oxygen-reduced air (8% oxygen, 92% nitrogen).

Figure 1. The full diameter core (Core J1) picture.

Table 1. Core parameter table.

Core Number	Permeability ($\times 10^{-3}$ μm^2)	Porosity (%)	Diameter (cm)	Length (cm)
J1	0.85	11.57	9.90	8.93
J27-1	0.87	13.94	2.51	3.51
J27-2	0.90	13.76	2.51	3.53

2.2. Experiment Equipment and Conditions

The main experimental equipment included a full-diameter core holder (temperature 0~150 °C, pressure 0~50 MPa), a Spec-RC035 large-scale nuclear magnetic resonance scanner, a confocal laser scanning microscope, a gas chromatography analyzer, a vacuum-saturation system, an ISCO pump, and a gas-liquid separation metering device. The specific experimental equipment and schematic diagrams are shown in Figures 2 and 3. The experimental temperature was 85 °C (formation temperature).

Figure 2. Full-diameter core holder (upper left) and Spec-RC035 large NMR scanner (upper right).

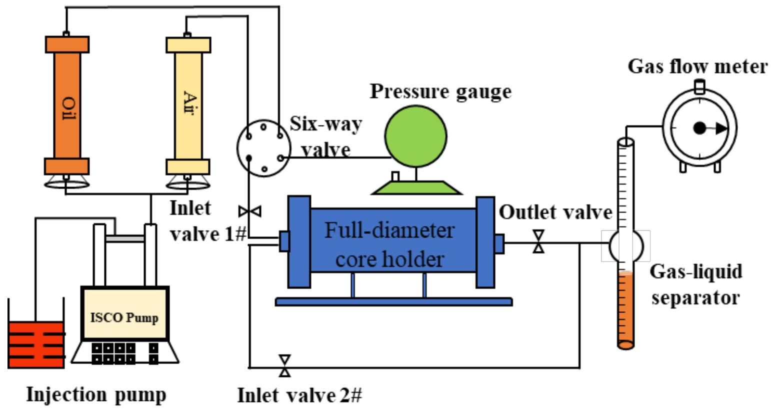

Figure 3. Flow diagram of air flooding/HnP experiments.

2.3. Experimental Procedures

Air flooding: The full-diameter core (Core J1) was placed in the holder (Figure 2) to simulate the formation environment (85 °C). To analyze the residual oil and produced oil, NMR scanning and GC analysis were carried out during the flooding experiment. The flooding experimental steps include: ① Vacuum the full-diameter core (Core J1) and saturate it with oil at high pressure, then calculate the saturated oil volume of the core. ② Conduct NMR scanning (T2, T1–T2) on the saturated core. ③ Load the core into the full-diameter core holder and connect the whole process according to Figure 3. ④ Open the inlet valve 1 and the outlet valve of the holder to carry out constant pressure 0.5 MPa air flooding. During this period, the produced oil and gas volumes were measured in real time, and the displacement was stopped when no oil was produced at the outlet. ⑤ After the displacement, the core was scanned again by NMR (T2, T1–T2) and the produced oil was analyzed by GC.

Air HnP: To eliminate the influence of the difference in the experimental core, the core used in the HnP experiment was the same as that used in the flooding experiment. Furthermore, NMR scanning and GC analysis were carried out during the HnP experiment. The HnP experimental steps include: ①–③ Refer to flooding experimental steps ①–③. ④ Close the outlet valve, open the inlet valve 1, and inject air at a constant pressure of 20 MPa until the internal pressure of the core is stable, then close the inlet valve 1 and soak for 24 h. ⑤ Open the inlet valve 2 and measure the produced oil and gas volumes in real time. The puff period is stopped when no oil and gas is produced at the inlet. ⑥ After HnP, the core is scanned again by NMR (T2, T1–T2) and the produced oil is analyzed by GC.

Core J27-1 is a core in the original state of saturated oil, and Core J27-2 is a core after gas flooding. Core J27-1 and Core J27-2 are only used for LSCM analysis, and the experimental method will not be repeated. The specific experimental design is shown in Table 2.

Table 2. Experimental design table.

Number	Core Number	Development Model	Injection Pressure/MPa
1	J1	Air flooding	0.5
2		Air HnP	20
3	J27-1	/	/
4	J27-2	Air flooding	0.5

3. Results and Discussion

3.1. Development Dynamics

Figures 4 and 5 show the production curve of constant pressure air flooding in the full-diameter core at different times and at different pore volume numbers (PV). During the large multiple air flooding process, the oil production rate shows an "L"-shaped decrease, the gas/oil ratio (GOR) rapidly increases, and the ultimate recovery factor can reach 23.36%. It can be seen that the gas breakthrough time is early (0.03 PV), which results in a long follow-up oil recovery cycle (16 PV), reflecting that strong heterogeneity of the reservoir and high gas/oil mobility ratio would lead to severe gas channeling during shale oil air flooding. When the injection volume reaches 10.6 PV, the recovery reaches 21.58%, and the GOR significantly rises to over 1100 m^3/m^3, resulting in a poor subsequent air flooding effect. Overall, it can be seen that the gas/oil replacement efficiency of air flooding is low, and adequate air injection ($\geq$10.6 PV) should be guaranteed to achieve a certain recovery factor.

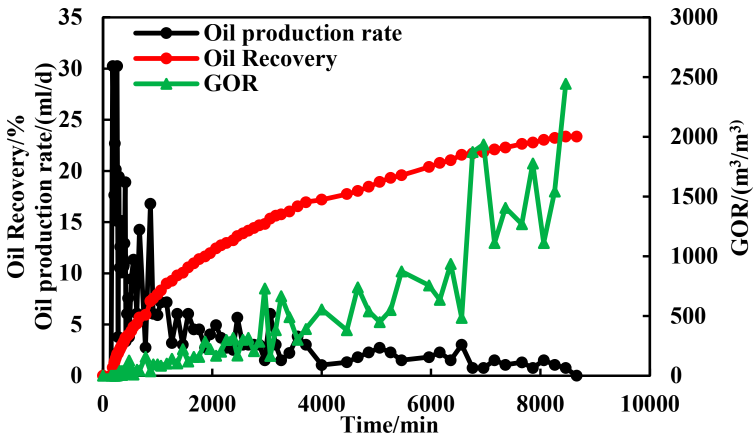

Figure 4. Production parameters of air flooding at different times.

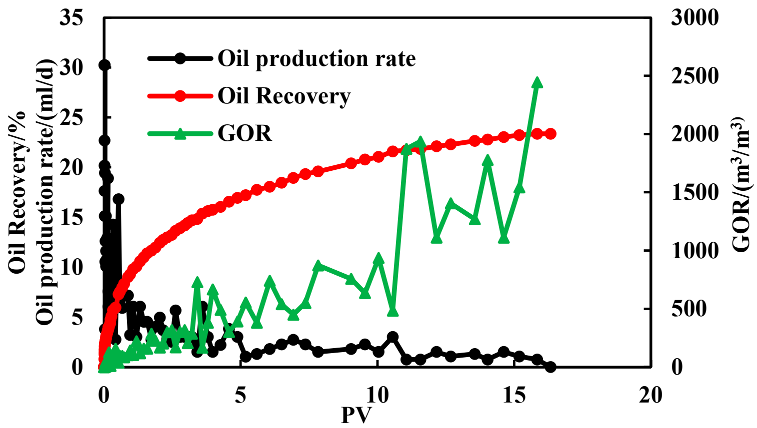

Figure 5. Production parameters of air flooding at different PV numbers.

Figure 6 shows the production curve of air HnP in the full-diameter core at different times. Different from air flooding, there is a gas backflow stage in the early period of the puff period. At this time, only gas is discharged and basically no oil is produced, although the formation energy is sufficient and rapidly decreasing. As the subsequent proximal gas is continuously expelled, the oil phase gradually recovers at a relatively low GOR (50–660 m^3/m^3). Therefore, air HnP development presents the characteristics of first producing gas and then producing oil. As a result, the GOR is high first and then low, and the oil production rate is first low and then high. Compared with air flooding, the air volume required for air HnP is also smaller, and the development time is significantly shorter (8660–270 min). Obviously, it takes more time (about 1500 min) for air flooding to achieve the same recovery factor (10.28%) of the first round of HnP. Therefore, it can be concluded that, in shale oil development, HnP development is conducive to more rapid oil production.

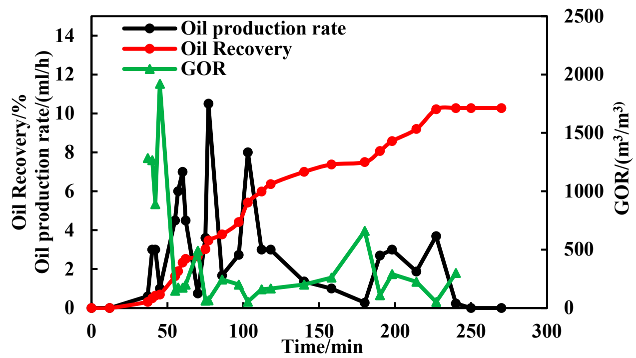

Figure 6. Production parameters of air HnP at different times.

Figure 7 shows the recovery factor of three rounds of air HnP. It can be seen that the first round of HnP has the highest recovery factor (10.28%), and the recovery factor of the subsequent two rounds is significantly lower (3.84%, 3.05%). Obviously, HnP mainly extracts the nearby oil and has a limited ability to recover the distal oil, which leads to the best effect of the first round of HnP and a rapid deterioration in the subsequent rounds. HnP presents a high oil recovery efficiency at the early development stage, while in the subsequent stages, the oil recovery efficiency rapidly decreases. Meanwhile, the cumulative recovery factor of three rounds of air HnP could reach 17.17%, lower than that of air flooding.

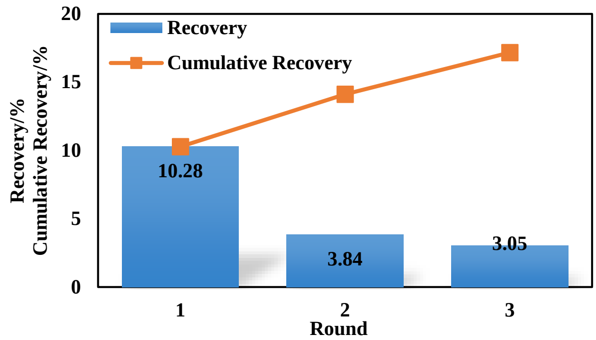

Figure 7. Recovery factors of three rounds of air HnP.

Notably, Yu (2016) concluded, by comparing the results of N_2 flooding and HnP experiments, that gas injection HnP is superior to the gas flooding in shale cores [20], which is not consistent with the results of this paper. By further analysis, we can conclude that the difference in conclusions is mainly due to the different conditions of the HnP experiments, especially the difference in the method of gas injection. In the previous paper, gas was injected into the core from both sides of the holder, providing more nearby oil, while it was injected at one side in this paper, which obviously explains the more effective HnP effects in the previous paper. Moreover, this phenomenon also confirms that HnP is more favorable in extracting the nearby oil and has a limited ability to recover the distal oil.

In summary, for air flooding, the compactness of the shale oil reservoir results in a long development time, while for air HnP, it is more conducive to the efficient recovery of nearby oil, but has limited ability to extract distal oil. It seems to be an ideal development model by which to rapidly recover nearby oil through HnP in the early stage of shale oil development, and then further initiate the distal oil by conducting flooding in the later stage, since larger-contact-area gas chambers [25] in the near-well zone formed by HnP should be conducive to the realization of flooding.

3.2. Residual Oil Analysis

To analyze the oil in Core J1 in different states, NMR scans were performed on the core before and after air injection development. Figure 8 shows the NMR T_2 spectrum and the cumulative oil ratio of the core after oil saturation, air flooding, and HnP (according to the experimental recovery factor, we corrected the signal amplitude of the T_2 spectrum to a certain extent). It can be seen that the main oil produced by air injection development mainly comes from large pores (>10 ms), while the oil in small pores (<1 ms) cannot be effectively extracted. After air injection development, more than 54% of the initial oil is still in medium pores (1–10 ms), which are the main concentrations of residual oil, accounting for 66% of the residual oil.

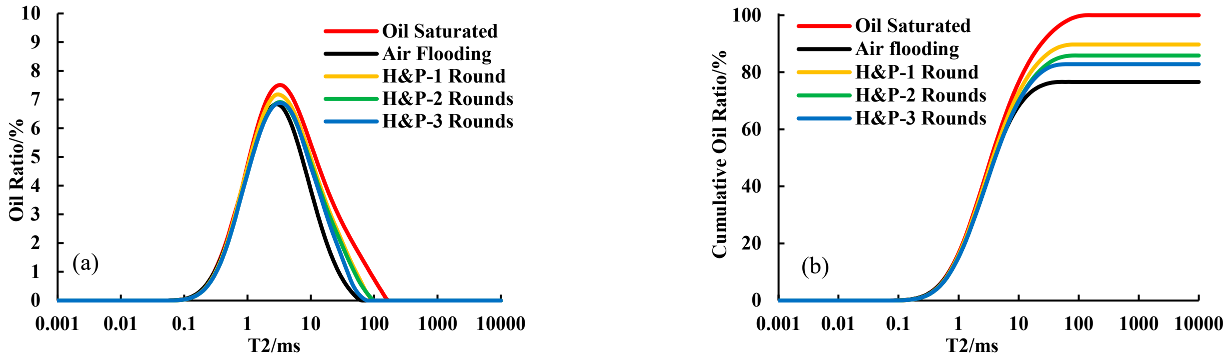

Figure 8. T_2 spectrum of Core J1 before and after air injection (**a**) and the cumulative oil volume proportion (**b**).

Figure 9 further quantifies the distribution of the oil phase in pores of different grades and their contribution to the recovery factor. In the initial state, the ratios of oil in small, medium, and large pores are 11.91%, 64.61%, and 23.48%, respectively. Obviously, the amount of oil in small pores before and after air injection development is basically unchanged (11.91–10.84%), indicating that it is difficult to extract the oil in small pores during air injection development. For air flooding, there is some reduction in medium pores oil (64.61–56.65%), with a corresponding recovery contribution of 7.96%, while oil in large pores is significantly reduced (23.48–8.45%), with a corresponding recovery contribution of 15.03%. Compared with air flooding, the oil reduction in medium and large pores after three rounds of HnP development is smaller; the recovery contribution in large pores is only 10.38%, resulting in a lower recovery. Therefore, it can be obtained that there is less oil in large pores, but it contributes more than 60% of the recovery factor of air injection development.

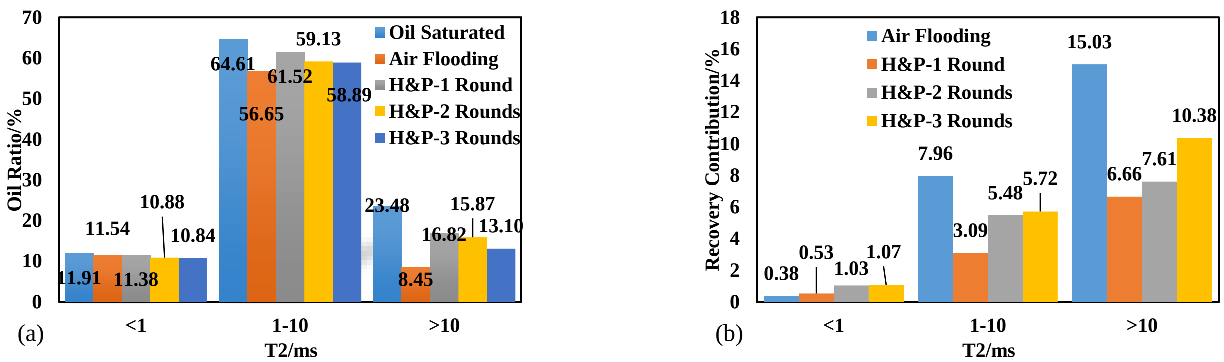

Figure 9. Distribution of oil in different grades of pores (**a**) and their contribution to recovery factor (**b**).

In conclusion, air injection development mainly extracts the oil in large pores, followed by medium pores, and it is difficult to recover the oil in small pores. Air HnP would be a more feasible and efficient development model in the early stages of shale oil development, while air flooding could achieve a higher recovery with high-intensity displacement. To combine the advantages of the two development modes, it seems to be a good choice to carry out HnP in the early stage to achieve rapid oil production, and then carry out air flooding in the later stage to further enhance the oil recovery.

To clarify the effect of air injection on the composition of oil in the core, two-dimensional nuclear magnetic resonance (2D NMR) scans were further carried out on the core in different states [31,32]. The T_1 and T_2 values can be obtained as follows; where T_{1S} and T_{2S} are surface relaxations, T_{1B} and T_{2B} are bulk relaxations, and T_{1D} and T_{2D} are diffusion relaxations.

$$\frac{1}{T_1} = \frac{1}{T_{1S}} + \frac{1}{T_{1D}} + \frac{1}{T_{1B}}$$

$$\frac{1}{T_2} = \frac{1}{T_{2S}} + \frac{1}{T_{2D}} + \frac{1}{T_{2B}}$$

The results of previous studies have shown that, as the viscosity of the oil phase increases (more heavy components, such as asphaltene), the T_2 value would decrease to a certain extent, while the change in T_1 value is relatively small [33,34], so the difference in light and heavy components in the oil phase can be judged based on the magnitude ratio of the T_1/T_2. In general, the larger the T_1/T_2 ratio, the higher the viscosity of the oil phase and the higher the content of heavy components [35–38].

The 2D NMR maps were further obtained by drawing a contour plot combining the T_1 and T_2 curves. Figure 10 shows the 2D NMR map of Core J1 in a saturated oil state. Several T_1/T_2 ratio lines are plotted in Figure 10, and it can be seen that the T_1/T_2 ratio in the upper left part of the two-dimensional spectrum is larger, which also represents the heavier components in the oil phase.

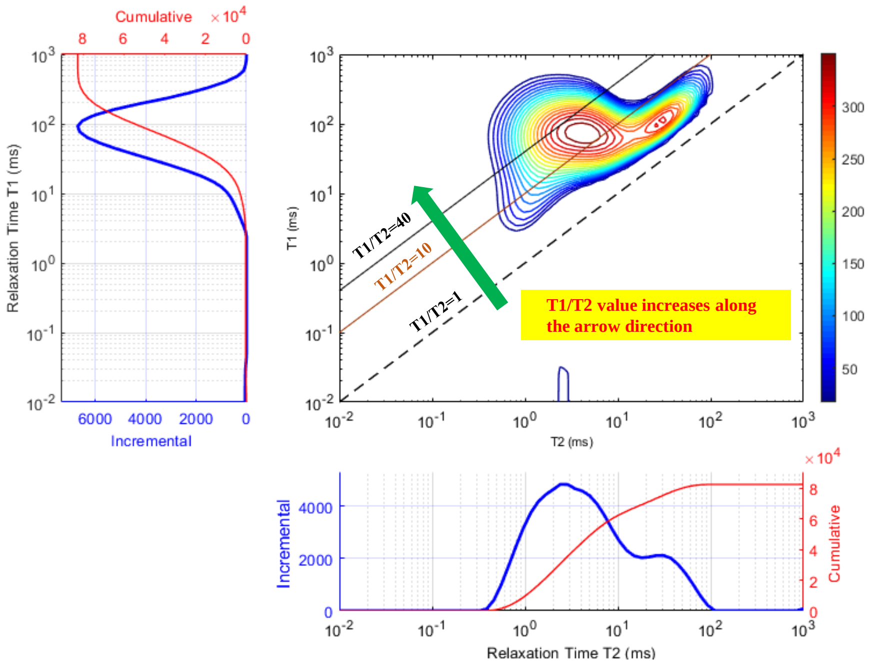

Figure 10. 2D NMR map of Core J1 in the saturated oil state. The blue line corresponds to the signal value increment, and the red line corresponds to the cumulative signal value.

Figure 11 shows the 2D NMR maps of Core J1 in three different states: saturated oil, after air flooding, and after three rounds of air HnP. The middle position of the double peak of the 2D NMR map of Core J1 in the saturated oil state, which is at the T_1/T_2 ratio of 8, is used as the dividing line (black dashed line in Figure 11) so that we can see the characteristics of the relative light and heavy components of the oil phase in the core, respectively. Obviously, there is a significant reduction in both the light component (upper left of the dashed line) signal amplitude and heavy component (lower right of the dashed line) signal amplitude of the oil phase after the air injection development, reflecting that the air injection development can achieve effective utilization of light and heavy components.

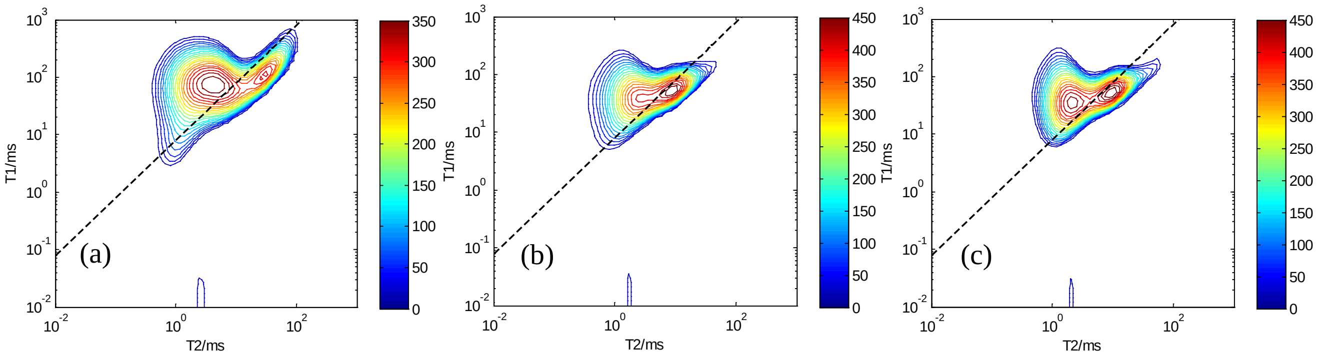

Figure 11. 2D NMR spectrum of Core J1 at three different states ((**a**) saturated oil; (**b**) after air flooding; (**c**) after three rounds of air HnP).

Figure 12 further shows the quantitative results of the respective proportions of light and heavy components in the core, and their corresponding recovery factors. Figure 12a shows that after air flooding and three rounds of HnP, the proportion of heavy components in the residual oil increases from 62.64% to 66.91% and 64.95%, respectively, which indicates that more light components are extracted during air injection development. Figure 12b also confirms that the recovery of light components is relatively high (22.3–32.11%), while the recovery of heavy components is relatively low (14.11–18.14%). Compared with HnP, the difference between light component recovery and heavy component recovery after air flooding is larger, which may be the result of a larger swept area and more abundant oxygen.

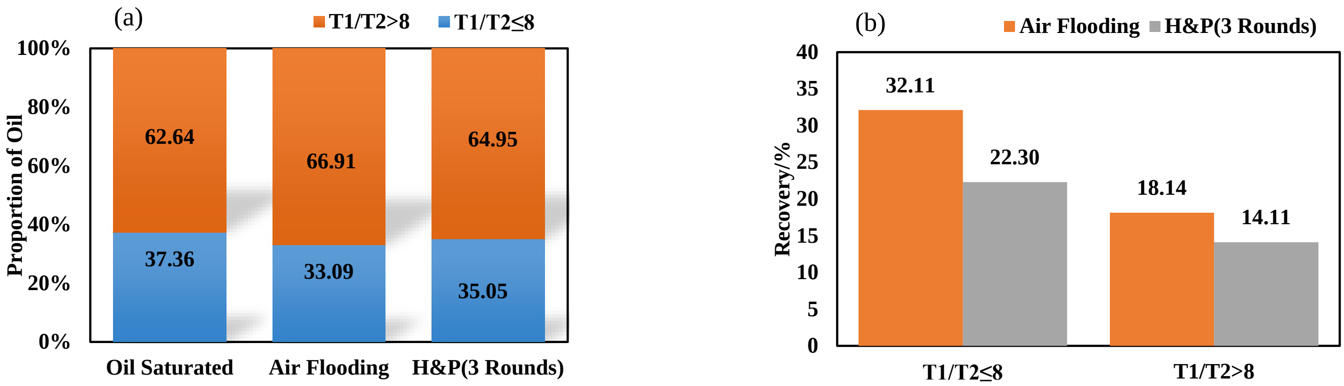

Figure 12. Respective proportions of light and heavy components (**a**) and the corresponding recovery factors (**b**).

To further clarify the distribution characteristics of light and heavy components of oil in shale cores in different states, two cores (Core J27-1: 0.87 × 10^{-3} μm^2; Core J27-2: 0.90 × 10^{-3} μm^2) with similar physical properties were prepared, one of which was an oil saturated core and the other was a core after air flooding. Two slices were taken from the two cores, and LSCM was performed on both slices. Figure 13 shows the LSCM results of the core slices before and after air flooding. The red regions of the figure represent the light components; the blue regions represent the heavy components; and the pink regions are the superposition of the two.

Figure 13a,b shows the LSCM image of the slice from the oil-saturated core (Core J27-1) and its corresponding 3D reconstruction image. It can be seen that, in the initial state, light and heavy components in large pores are basically overlapped, while small pores are mainly dispersed heavy components. On the whole, the content of light and heavy components in the core after air flooding is 7.52% and 7.47%, and the content ratio of light to heavy components is 1.006. Figure 13c,d shows the LSCM image of the slice from the core (Core J27-2) after air flooding and its corresponding reconstruction image. It can be seen that, after air flooding, the proportion of heavy components in the residual oil significantly increases (the oil color changes from pink to blue), which means more light components in large pores are recovered, while more heavy components are adsorbed on the surface of large pores, leading to a lower recovery factor of heavy components. Meanwhile, more heavy components distributed in small pores also make it more difficult for them to be extracted. As a result, the content of light and heavy components in the core after air flooding is 5.23% and 6.83%, respectively, and the content ratio of light to heavy components decreases to 0.7657.

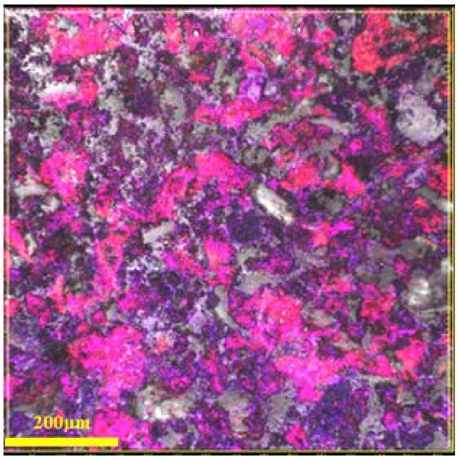

(a) LSCM image of oil saturated slice

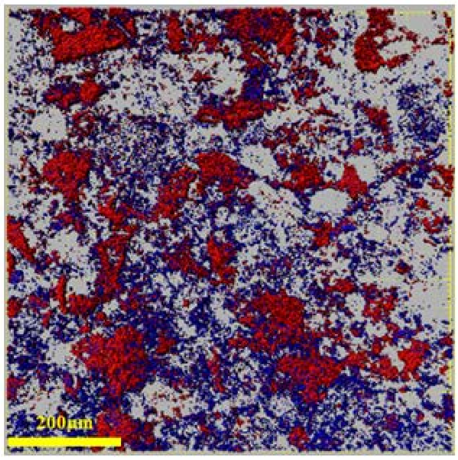

(b) Reconstruction image of oil saturated slice

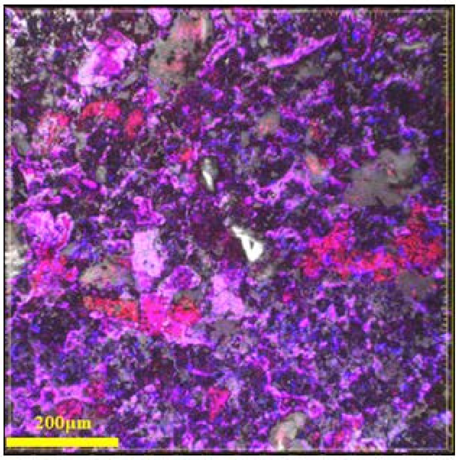

(c) LSCM image of slice after air flooding

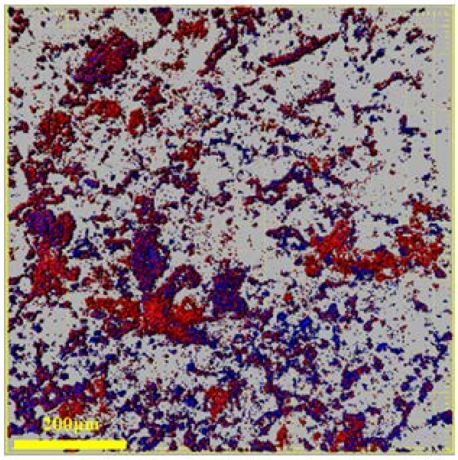

(d) Reconstruction image of slice after air flooding

Figure 13. LSCM images of slices in different states and the corresponding reconstruction images. (Red regions: light components of crude oil, which may include pyrolysis gas (<nC12), gasoline (nC10–nC16) and some kerosene (nC11–nC19); blue regions: heavy components of crude oil, which may include some Kerosene (nC11–nC19), diesel (nC14–nC22), heavy oil (nC16–nC26); Pink regions: the superposition of light and heavy components; Black regions: the matrix.).

It can be seen from the results of 2D NMR and LSCM that the residual oil in the core does show a decrease in the proportion of light components and an increase in the proportion of heavy components after air injection development.

3.3. Produced Oil Analysis

In order to clarify the effect of air injection development on the components of produced oil, GC analysis was carried out on three kinds of oil, including initial saturated oil, oil produced by air flooding, and oil produced by air HnP. As can be seen from Figure 14, the oil produced by air injection development has a relatively higher content of low carbon number hydrocarbons (C_{15-}) and a relatively lower content of high carbon number hydrocarbons (C_{15+}) compared to crude oil, and the impact of gas flooding is more obvious than by HnP. The difference between the total hydrocarbon distribution of produced oil and initial oil shows that the recovery efficiency of different components is different in air injection development, which is consistent with the experimental results above.

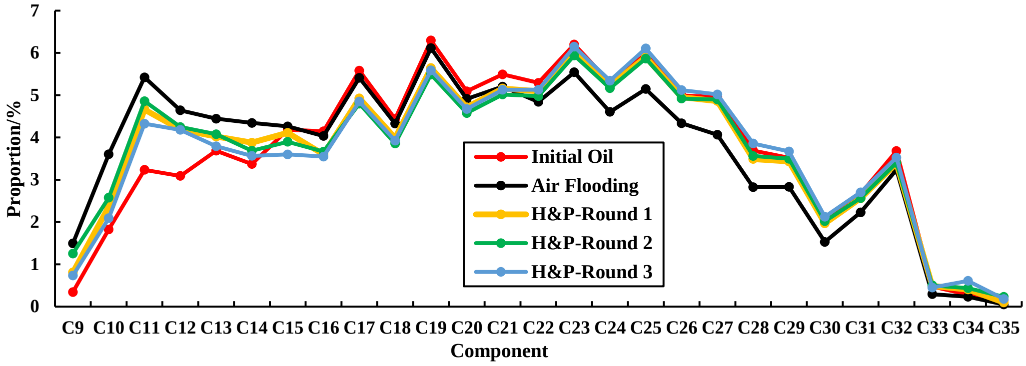

Figure 14. GC results of initial oil and produced oil.

A clear conclusion can be drawn by combining the results of NMR, LSCM, and GC analysis; that is, air injection is more adequate for the mobilization of the lighter components of the oil. As for the impact of air flooding being greater than HnP, this is believed to be due to the flooding sweeping a larger volume and recovering more oil.

4. Conclusions

We conducted various experiments to elucidate the effectiveness of air flooding and air HnP in enhancing the recovery of the shale oil reservoir of the Lucaogou Formation in the Jimsar area. The conclusions were as follows:

(1) For the Jimsar shale oil reservoir, air flooding is characterized by an early gas breakthrough, a rapid increase in GOR, and an "L" shape oil production decline. To achieve a certain recovery factor, adequate air injection (≥10.6 PV) should be guaranteed, and the ultimate recovery factor of large PV (16 PV) air flooding can reach 23.36%.

(2) In contrast to air flooding, air HnP presents characteristics of first producing gas and then producing oil. The GOR is high first and then low, and the oil production rate is first low, then high. The recovery factor of the first round of HnP accounts for 60% of the cumulative recovery factor of the three rounds of HnP, indicating a rapid decrease in recovery factor with increasing HnP rounds. The air volume required for the first round of air HnP is smaller and the development time is significantly shorter, although the cumulative recovery factor (17.17%) of the three rounds of HnP is lower than that of air flooding. Consequently, air HnP seems to be a more feasible and efficient development model for nearby oil in the shale reservoir, while a higher final recovery factor can be achieved through air flooding due to its large swept volume.

(3) As shown from the NMR results, the oil in large pores (>10 ms) accounts for only 23.48% of the total oil volume under initial conditions, but contributes more than 60% of the recovery factor from air injection development, while the oil in small pores is difficult effectively extract. It is mainly the difference in the degree of oil recovery in large pores that leads to the difference in air flooding recovery and air HnP recovery. After air injection development, more than 54% of the initial oil is still in medium (1–10 ms) pores, which are the main concentrations of residual oil, accounting for more than 66% of the residual oil.

(4) Air injection development has a higher recovery factor for light components (C_{15-}), which will lead to an increase in the content of heavy components (C_{15+}) in residual oil, and the development effectiveness of gas flooding is more obvious than air HnP.

(5) Based on the 2D NMR data, the distinction and quantitative analysis of light and heavy components of oil in cores can be realized, which provides a new approach to

analyze oil properties in porous media, and a systematic method was established to evaluate the development effectiveness of air injection in shale oil.

Author Contributions: Methodology, C.C., X.T., X.C. and Z.L.; Software, X.T. and R.Z.; Formal analysis, G.L.; Investigation, H.Q.; Data curation, M.Q., R.Z. and Z.D.; Writing—original draft, X.T.; Writing—review and editing, C.C., X.C. and Z.L.; Supervision, Y.L.; Project administration, M.Q. All authors have read and agreed to the published version of the manuscript.

Funding: This research received no external funding.

Data Availability Statement: Not applicable.

Conflicts of Interest: The authors declare no conflict of interest.

References

1. Dong, C.; Hoffman, B.T. Modeling gas injection into shale oil reservoirs in the sanish field, North Dakota. In Proceedings of the Unconventional Resources Technology Conference, Denver, CO, USA, 12–14 August 2013; Society of Exploration Geophysicists, American Association of Petroleum Geologists, Society of Petroleum Engineers: Tulsa, OK, USA, 2013; pp. 1824–1833.
2. Yu, W.; Al-Shalabi, E.W.; Sepehrnoori, K. A sensitivity study of potential CO_2 injection for enhanced gas recovery in Barnett shale reservoirs. In Proceedings of the SPE Unconventional Resources Conference, The Woodlands, TX, USA, 1–3 April 2014.
3. Sheng, J.J.; Chen, K. Evaluation of the EOR potential of gas and water injection in shale oil reservoirs. *J. Unconv. Oil Gas Resour.* **2014**, *5*, 1–9. [CrossRef]
4. Zhu, P.; Balhoff, M.T.; Mohanty, K.K. Simulation of fracture-to-fracture gas injection in an oil-rich shale. In Proceedings of the SPE Annual Technical Conference and Exhibition, Houston, TX, USA, 28–30 September 2015.
5. Kong, B.; Wang, S.; Chen, S. Simulation and optimization of CO2 huff-and-puff processes in tight oil reservoirs. In Proceedings of the SPE Improved Oil Recovery Conference, Tulsa, OK, USA, 11–13 April 2016.
6. Kokkinos, N.C.; Nkagbu, D.C.; Marmanis, D.I.; Dermentzis, K.I.; Maliaris, G. Evolution of Unconventional Hydrocarbons: Past, Present, Future and Environmental FootPrint. *J. Eng. Sci. Technol. Rev.* **2022**, *15*, 15–24. [CrossRef]
7. Sheng, J. *Enhanced Oil Recovery in Shale and Tight Reservoirs*; Gulf Professional Publishing: Houston, TX, USA, 2019.
8. Alfarge, D.; Wei, M.; Bai, B. Air injection in shale and tight oil reservoirs. In *Developments in Petroleum Science*; Elsevier: Amsterdam, The Netherlands, 2020; Volume 67, pp. 87–111.
9. Jia, H.; Yuan, C.-D.; Zhang, Y.-C.; Peng, H.; Zhong, D.; Zhao, J.-Z. Recent progress of high-pressure air injection (HPAI) process in Light Oil Reservoir: Laboratory investigation and field application. In Proceedings of the SPE Heavy Oil Conference Canada, Calgary, AB, Canada, 12–14 June 2012.
10. Jia, H. Investigation into the Oxidation Mechanism of Crude Oil and Gas Channeling Prevention for Application of High-Pressure Air Injection (HPAI) Process. Ph.D. Dissertation, Southwest Petroleum University, Sichuan, China, 2012.
11. Juan, E.; Sanchez, A.; Del Monte, A.; Moore, R.; Mehta, S.; Ursenbach, M. Laboratory Screening for Air Injection-Based IOR in Two Waterf looded Light Oil Reservoirs. *J. Can. Pet. Technol.* **2005**, *44*, 31–41. [CrossRef]
12. Gutierrez, D.; Kumar, V.; Moore, R.G.; Mehta, S.A. Air injection and waterflood performance comparison of two adjacent units in the Buffalo Field. *SPE Reserv. Eval. Eng.* **2008**, *11*, 848–857.
13. Youwei, J.; Yitang, Z.; Shangqi, L.; Wenlong, G.; Yaping, C.; Shuangmao, L. Displacement mechanisms of air injection in low permeability reservoirs. *Pet. Explor. Dev.* **2010**, *37*, 471–476. [CrossRef]
14. Li, J.; Mehta, S.; Moore, R.; Ursenbach, M.; Zalewski, E.; Ferguson, H.; Okazawa, N. Oxidation and ignition behaviour of saturated hydrocarbon samples with crude oils using TG/DTG and DTA thermal analysis techniques. *J. Can. Pet. Technol.* **2004**, *43*, 45–51. [CrossRef]
15. Huan, Q.I.; Yiqiang, L.I.; Xiaolong, C.H.; Anlin, L.O.; Li, W.E.; Jie, L.I.; Jianghao, L.U.; Xuebin, S.U.; Xiang, T.A.; Cuo, G.U. Low-temperature oxidation of light crude oil in oxygen-reduced air flooding. *Pet. Explor. Dev.* **2021**, *48*, 1393–1402.
16. Liu, G.; Zhang, T.; Xie, Q.; Liu, W.; Wang, L.; Yang, D. Experimental evaluation of live oil oxidation together with its physical properties during air injection in a tight oil reservoir. *Fuel* **2021**, *283*, 119121. [CrossRef]
17. O'Brien, W.J.; Moore, R.G.; Mehta, S.A.; Ursenbach, M.G.; Kuhlman, M.I. Performance of air injection vs. CO_2/water injection in a tight, light-oil reservoir: A laboratory study. *SPE Reserv. Eval. Eng.* **2019**, *22*, 1049–1062. [CrossRef]
18. Zhang, Y.; Huang, S.; Sheng, J.J.; Jiang, Q. Experimental and analytical study of oxygen consumption during air injection in shale oil reservoirs. *Fuel* **2020**, *262*, 116462. [CrossRef]
19. Jia, H.; Sheng, J.J. Discussion of the feasibility of air injection for enhanced oil recovery in shale oil reservoirs. *Petroleum* **2017**, *3*, 249–257. [CrossRef]
20. Yu, Y.; Li, L.; Sheng, J.J. A comparative experimental study of gas injection in shale plugs by flooding and huff-n-puff processes. *J. Nat. Gas Sci. Eng.* **2017**, *38*, 195–202. [CrossRef]
21. Bai, J.; Liu, H.; Wang, J.; Qian, G.; Peng, Y.; Gao, Y.; Yan, L.; Chen, F. CO_2, water and N2 injection for enhanced oil recovery with spatial arrangement of fractures in tight-oil reservoirs using huff-'n-puff. *Energies* **2019**, *12*, 823. [CrossRef]

22. Nguyen, P.; Carey, J.W.; Viswanathan, H.S.; Porter, M. Effectiveness of supercritical-CO_2 and N2 huff-and-puff methods of enhanced oil recovery in shale fracture networks using microfluidic experiments. *Appl. Energy* **2018**, *230*, 160–174. [CrossRef]
23. Lu, T.; Li, Z.; Li, J.; Hou, D.; Zhang, D. Flow behavior of N2 huff and puff process for enhanced oil recovery in tight oil reservoirs. *Sci. Rep.* **2017**, *7*, 15695. [CrossRef]
24. Yue, P.; Xie, Z.; Huang, S.; Liu, H.; Liang, S.; Chen, X. The application of N2 huff and puff for IOR in fracture-vuggy carbonate reservoir. *Fuel* **2018**, *234*, 1507–1517. [CrossRef]
25. Zou, B.; Pu, W.; Zhou, X.; Du, D.; Shi, Y.; Xia, W.; Zeng, F. Experimental study on the feasibility of nitrogen huff-n-puff in a heavy oil reservoir. *Chem. Eng. Res. Des.* **2022**, *184*, 513–523. [CrossRef]
26. Neng, G.A.O.; Jian, Z.; Jia, H.E. Application of hypoxic air huff and puff technology in deep heavy oil reservoirs in Lukeqin oilfield. *Xinjiang Pet. Geol.* **2020**, *41*, 748.
27. Jia, H.; Sheng, J.J. Simulation study of huff-n-puff air injection for enhanced oil recovery in shale oil reservoirs. *Petroleum* **2018**, *4*, 7–14. [CrossRef]
28. Tang, W.; Sheng, J.J. Huff-n-puff gas injection or gas flooding in tight oil reservoirs? *J. Pet. Sci. Eng.* **2022**, *208*, 109725. [CrossRef]
29. Li, L.; Su, Y.; Hao, Y.; Zhan, S.; Lv, Y.; Zhao, Q.; Wang, H. A comparative study of CO_2 and N_2 huff-n-puff EOR performance in shale oil production. *J. Pet. Sci. Eng.* **2019**, *181*, 106174. [CrossRef]
30. Song, Y.; Song, Z.; Zeng, H.; Tai, C.; Chang, X. N2 and CO_2 Huff-n-Puff for Enhanced Tight Oil Recovery: An Experimental Study Using Nuclear Magnetic Resonance. *Energy Fuels* **2022**, *36*, 1515–1521. [CrossRef]
31. Jun, W.; Xiaohai, M.; Weimin, W.; Naigui, L. 2D NMR distribution function for microscale remaining oil. *Pet. Geol. Exp.* **2015**, *37*, 654–659.
32. Zhang, X. *Experimental Study on Mechanisms of Chemical Flooding for Heavy Oil Reservoirs at Pore Scale Based on Two-Dimensional Spectrum Technology*; China Science: Beijing, China, 2020; p. 1.
33. Yang, Z.; Hirasaki, G.J.; Appel, M.; Reed, D.A. Viscosity evaluation for NMR well logging of live heavy oils. *Petrophys.-SPWLA J. Form. Eval. Reserv. Descr.* **2012**, *53*, 22–37.
34. Lo, S.-W.; Hirasaki, G.J.; House, W.V.; Kobayashi, R. Mixing rules and correlations of NMR relaxation time with viscosity, diffusivity, and gas/oil ratio of methane/hydrocarbon mixtures. *SPE J.* **2002**, *7*, 24–34. [CrossRef]
35. Korb, J.-P.; Nicot, B.; Louis-Joseph, A.; Bubici, S.; Ferrante, G. Dynamics and wettability of oil and water in oil shales. *J. Phys. Chem. C* **2014**, *118*, 23212–23218. [CrossRef]
36. Rylander, E.; Philip, M.S.; Jiang, T.; Lewis, R. NMR T_2 distributions in the Eagle Ford shale: Reflections on pore size. In Proceedings of the SPE Unconventional Resources Conference, The Woodlands, TX, USA, 10–12 April 2013.
37. Tinni, A.; Sondergeld, C.; Rai, C. NMR T_1–T_2 response of moveable and non-moveable fluids in conventional and unconventional rocks. In Proceedings of the International Symposium of the Society of Core Analysts, Avignon, France, 8–11 September 2014; pp. 8–11.
38. Fleury, M.; Romero-Sarmiento, M. Characterization of shales using T1–T_2 NMR maps. *J. Pet. Sci. Eng.* **2016**, *137*, 55–62. [CrossRef]